Korea-Australia Rheology Journal
Vol. 20, No. 3, September 2008 pp. 127-142

# Studying confined polymers using single-molecule DNA experiments

**Chih-Chen Hsieh[1] and Patrick S. Doyle[2,*]**
[1]*Department of Chemical Engineering, National Taiwan University*
[2]*Department of Chemical Engineering, Massachusetts Institute of Technology*

(Received April 23, 2008)

## Abstract

The development of fluorescence microscopy of single-molecule DNA in the last decade has fostered a bold jump in the understanding of polymer physics. With the recent advance of nanotechnology, devices with well-defined dimensions that are smaller than typical DNA molecules can be readily manufactured. The combination of these techniques has provided an unprecedented opportunity for researchers to examine confined polymer behavior, a topic far less understood than its counterpart. Here, we review the progress reported in recent studies that investigate confined polymer dynamics by means of single-molecule DNA experiments.

***Keywords*** **:** confined polymer, single-molecule DNA, tube-like confinement, silt-like confinement, surface confinement, blob theory

## 1. Introduction

Polymer behavior under confinement has long been a research interest due to its fundamental and practical importance. The applications include various separation processes, oil extraction from porous media and genomics assays. To foster understanding in this area, scaling theories and deterministic predictions for polymers under different degrees of confinement have been proposed for years (Daoud and de Gennes, 1977; Odijk, 1983). However, experimental studies of confined polymer behavior mostly focused on investigating the partition function and the retarded transport for weakly confined chains with the ratio of the radius of gyration ($R_{g,bulk}$) over the smallest dimension of confinement ($h$) between 0.1 to 1.

The review of Gorbunov and Skvortsov (1995) has summarized the theoretical predictions of partition function of confined polymers with emphasis on the situation with polymer adsorption on the surface of confinement. On the other hand, Teraoka (1996) has reviewed both the theoretical predictions and experimental measurements of the partition function and the retarded diffusion of confined polymers. The experiments were typically carried out with size-exclusion chromatography to determine partition coefficient, and with membrane filtration and dynamic light scattering to determine diuffsion coefficient. The transport of weakly confined polymers in hydrodynamic flows was reviewed by Deen (1987) and Dechadilok and Deen (2006). Since polymer conformation was assumed to be only weakly perturbed, their transport was considered as a variation of hindered transport of spherical particles. Shaqfeh recently published a thorough review(Shaqfeh, 2005) of single DNA dynamics in flow. It is interesting to note that the section on confined DNA dynamics focused more on simulations than experiments, which accurately reflected the state of the field at that time.

The disparity between the progress in theories and experiments reflected the difficulty in performing these experiments. Such impediments are mainly due to (i) the inability to create uniform features that are small enough to confine synthesized polymers (a polystyrene molecule of MW = $10^6$ has $R_{g,bulk} \sim 30$ nm) while at the same time to allow an accurate measurement of polymer properties, (ii) the polydispersed nature of synthesized polymers, and (iii) the difficulty to decouple effects of the partition coefficient and retarded transport coefficient in experimental results. However, the advance in single-molecule fluorescence microscopy with DNA molecules(Perkins *et al.*, 1994; 1995) and the development of nanotechnology in the last ten years makes it possible to directly observe and measure the behavior of DNA as a model polymer in well-defined strong confinement(Volkmuth and Austin, 1992; Volkmuth *et al.*, 1994). Therefore, this review focuses on the recently gained understanding of strongly confined polymers ($R_{g,bulk}/h > 1$) using single-molecule DNA experiments. We consider polymers confined in a slit-like geometry, in a circular or a rectangular pore, and on a surface. Studies of polymers passing through a confining pore, although highly related to the current topic, will not be covered.

*Corresponding author: pdoyle@mit.edu

The studies of confined DNA have also lead to new approaches in many applications including separation of biomolecules(Han *et al.*, 1999; Han and Craighead, 2000; 2002; Cabodi *et al.*, 2002; Stein *et al.*, 2006; Cross *et al.*, 2007; Salieb-Beugelaar *et al.*, 2008), rapid gene-mapping (Riehn *et al.*, 2005; Jo *et al.*, 2007; Chan *et al.*, 2004; Larson *et al.*, 2006), and understanding DNA-protein interactions (Wang *et al.*, 2005). Several recent articles (Tegenfeldt *et al.*, 2004b; Eijkel and van den Berg, 2005; Mannion and Craighead, 2007; Douville *et al.*, 2008; Han *et al.*, 2008) have provided excellent reviews on these subjects and are complementary to the current review.

The article is organized as follows. First, we define the three types of confinement to be discussed. Second, we summarize the theories that are used to explain/predict the confinement effects on DNA/polyelectrolytes. Related simulation results are also briefly reviewed here. Third, we overview recent findings on confined DNA behavior at equilibrium. Ionic effects and non-equilibrium dynamics of confined DNA are also discussed. At the end, the outlook for future research is given.

## 2. Type of confinement

We define "confined" in this article as the situation when a polymer is placed in a geometry that has at least one dimension smaller than the polymer's equilibrium size in a dilute bulk solution $\sim R_{g,bulk}$. Following this thought, we define three major types of confinement. *Slit-like* confinement is defined when only one dimension of the geometry is smaller than the natural size of a polymer ($h < R_{g,bulk}$). Similarly, *tube-like* confinement is defined when a polymer is confined in a tube with a diameter $h < R_{g,bulk}$. In reality, this type of confinement is usually realized as a rectangular channel with its height ($h$) and width ($d$) smaller than $R_{g,bulk}$. *Surface* confinement is defined when a polymer is limited to move in a plane. Fig. 1 illustrates these three types of confinement, the relevant theories, and representative fluorescence images of confined λ-DNA. From the fluorescence images in Fig. 1 one can get a feel for the striking conformational changes induced by confinement.

Other types of confinements also exist in addition to those mentioned above. For example, it is possible to confined a chain from all three dimensions to form a box-like confinement (Sakaue and Raphael, 2006). A polymer passing through a point-like pore can be considered as a slip-link type confinement (Kasianowicz *et al.*, 1996; Lubensky and Nelson, 1999). Some studies actually involved these two types of confinements (Nykypanchuk *et al.*, 2002; 2005), and such combination is common in many bio-

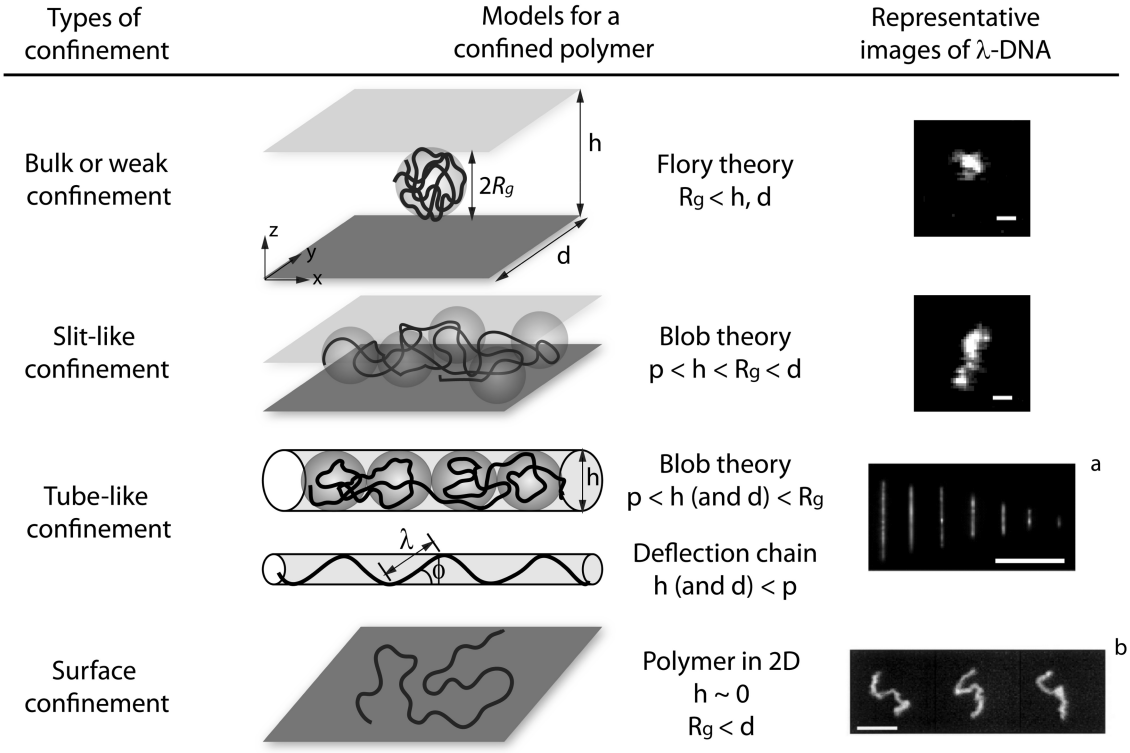


**Fig. 1.** Illustrations and theoretical models for different types of confinement, and representative fluorescence images of λ-DNA in corresponding confinement. $h$ and $d$ are the height (or diameter) and the width of the confinement. $p$ is the persistence length of DNA molecule. The scale bars in fluorescence images are (from top to bottom) 1, 1, 10, 10 μm, respectively. a. Reprinted with permission from Reisner *et al*. Phys. Rev. Lett., Copyright 2005 American Physical Society; b. Reprinted with permission from Maier and Rädler Phys. Rev. Lett., Copyright 1999 American Physical Society.

logical processes in cells. While they are interesting and important, in this article we limit our scope to the confinements listed in Fig. 1 because of their similarity from the viewpoint of resulting effects on DNA/linear polyelectrolytes.

## 3. Theories

We summarize two theories that were proposed to describe confined chain behavior: de Gennes' blob theory (de Gennes, 1976; Brochard, 1977; Brochard and de Gennes, 1977; Daoud and de Gennes, 1977) for $p << \min\{h,d\} << R_g$ and Odijk's deflection chain theory (Odijk, 1983) for $h,d << p$. Blob theory can be applied to both slit-like and tube-like confinements, while the original deflection chain model is limited to tube-like confinement (see Fig. 1). The two theories predict very different scalings for confined DNA conformation and dynamics. Further, the transition between the two regimes is still not well understood.

### 3.1. Blob theory

The concept of the "blob" was proposed by de Gennes to facilitate the understanding of concentrated polymer solutions and melts, and later extended to describe polymers in confinement due to the similarity between these problems. The blob theory for a confined polymer with excluded volume can be condensed to the following arguments. (1) The chain can be thought of as a string of blobs with each blob having a diameter $h$. Chain segments in blobs are not aware of the presence of the confinement and follow a 3D self-avoiding walk (SAW). (2) The blobs follow a 2D SAW in slit-like confinement and a 1D SAW in tube-like confinement. (3) Hydrodynamic interactions are screened at a length scale of h and therefore hydrodynamic interactions between blobs are negligible. (4) Chain segments within blobs interact hydrodynamically and therefore each blob can be considered non-draining.

The arguments (1) and (2) define the polymer conformation in confinement, and can also be obtained using Flory's variational approach. The arguments (3) and (4) provide principles for estimating the drag coefficient and therefore the dynamic properties of a confined chain. To reach the scaling predictions given by blob theory for a confined DNA, we first consider the equilibrium size ($R_{bulk}$) of an unconfined, semiflexible polymer in a good solvent. From Flory theory (Rubinstein and Colby, 2003),

$$R_{bulk} \sim v^{\frac{1}{5}} b^{\frac{2}{5}} N^{\frac{3}{5}} \sim L^{\frac{3}{5}} (pw)^{\frac{1}{5}} \tag{1}$$

where $N$ is the total number of statistical segments in a DNA, $p$ the persistence length of a semiflexible chain (representing the local stiffness of the chain), $w$ the effective diameter of the polymer, $v \approx wp^2$ the excluded volume (EV) of a statistical segment, and $L=2pN$ the contour length. The Kuhn length $b$ is twice the persistence length. Following the argument (1) and Eq. (1), a blob with a diameter equal to $h$ contains $g \sim h^{\frac{5}{3}} w^{-\frac{1}{3}} p^{-\frac{4}{3}}$ segments, and a chain consists of $N_b = N/g$ blobs. The scalings of the nominal sizes of confined chains in a slit ($R_{slit}$) and in a tube ($R_{tube}$) can be obtained using the argument (2):

$$R_{slit} \sim hN_b^{\frac{3}{4}} \sim L^{\frac{3}{4}} h^{-\frac{1}{4}} (pw)^{\frac{1}{4}} \tag{2}$$

$$R_{tube} \sim hN_b \sim Lh^{-\frac{2}{3}} (pw)^{\frac{1}{3}} \tag{3}$$

The scalings have been tested by Monte Carlo simulations (Wall *et al.*, 1978; Milchev and Binder, 1996). The drag coefficient of a confined chain $\zeta_{chain}$ can be estimated using the arguments (3) and (4):

$$\zeta_{chain} \sim \eta h N_b \sim \eta L h^{-\frac{2}{3}} (pw)^{\frac{1}{3}}. \tag{4}$$

Here $\eta$ is the solvent viscosity. Having $\zeta_{chain}$, the longest relaxation time $\tau_1$, and the diffusivity $D$ can be subsequently derived. For a polymer in a slit-like confinement,

$$D_{slit} \sim \frac{k_B T}{\zeta_{chain}} \sim \eta^{-1} L^{-1} h^{\frac{2}{3}} (pw)^{-\frac{1}{3}} \tag{5}$$

$$\tau_{1,slit} \sim R_{slit}^2 / D_{slit} \sim \eta L^{\frac{5}{2}} h^{-\frac{7}{6}} (pw)^{\frac{5}{6}} \tag{6}$$

For DNA in tube-like confinement (Brochard and de Gennes, 1977; Tegenfeldt *et al.*, 2004a),

$$D_{tube} \sim \eta^{-1} L^{-1} h^{\frac{2}{3}} (pw)^{-\frac{1}{3}} \tag{7}$$

$$\tau_{1,tube} \sim R_{tube} h / D_{tube} \sim \eta L^2 h^{-\frac{1}{3}} (pw)^{\frac{2}{3}}. \tag{8}$$

Note that the predicted scalings of DNA diffusivity in slit and tube confinements are the same, but the prefactors will be different. For a rectangular channel as a tube-like confinement, the effective tube diameter $h_{av}$ is usually taken as the geometric average of the channel depth and height (Reisner *et al.*, 2005).

We remark that de Gennes' original derivation dealt with a flexible chain in a good solvent where $v \approx b^3$ because $b \approx w$ for flexible polymers (Rubinstein and Colby, 2003). Replacing $pw$ terms with $b^2$ recovers de Gennes' original predictions. In addition to the above scaling arguments, Harden and Doi (1992) have provided a deterministic prediction of the diffusivity of a polymer confined in a tube. The boundary-mediated hydrodynamic interactions were considered in their calculation. For polymers in a good solvent, they predicted $D \sim N^{-1} h^{0.61}$, depending less strongly on $h$ than predicted in Eq. (7).

Studies of Jendrejack *et al.* (2003a; 2003b) using Brownian dynamics simulations with boundary-mediated hydro-

dynamic interactions, estimated by finite-element methods, found $R \sim h^{-2/3}$, $\tau_1 \sim h^{-1/3}$, and $D \sim h^{1/2}$ for DNA confined in a square channel. The former two scalings are the same as blob theory predictions, while the latter one is closer to the prediction of Harden and Doi. Similar simulations of Chen *et al.* (2004) for confined DNA in a slit yielded $R \sim h^{-1/4}$ and $D \sim h^{2/3}$, the same as blob theory predictions. The same scaling for $D$ was also found by Usta *et al.* (2005) using the Lattice Boltzmann method.

### 3.2. Deflection chain theory

Although the condition of $p << h$, $d$ is almost always true for flexible polymers, it can be violated when semiflexible polymers with long orientational memory are confined. Odijk (1983) addressed this issue by considering a semiflexible chain placed in a tube-like pore. For an unconfined semiflexible chain, the mean-square average deviation from its starting end has been well known as $<\varepsilon^2(s)>= 2s^3/3p$. Here $s$ is the arc length position along the contour. If this chain is placed at the center of a tube-like confinement with diameter $h << p$, it will hit the wall at $\varepsilon(\lambda) \approx h/2$ and must change the direction. Odijk defined this new length scale $\lambda \approx (h^2 p)^{1/3}$ as the deflection length. Since $\lambda << p$, the semiflexible chain segment of a length $\lambda$ can be thought as a rigid rod, and the whole chain can be considered as a link of $L/\lambda$ rigid rods deected by the boundary along the tube (see Fig. 1). The extension of the chain can be estimated:

$$R_{Odijk} = L\cos\phi \approx L[1-(h/\lambda)^2] = L\left[1-\alpha_o\left(\frac{h}{p}\right)^{2/3}\right] \quad (9)$$

where $\phi$ is the angle between a deflection segment and the tube wall (see Fig. 1) and $\alpha_o$ is a proportionality constant that has recently been evaluated to be $0.1701 \pm 0.0001$ (Burkhardt, 1995; Yang *et al.*, 2007). In a square/rectangular channel with height $h$ and width $d$ both smaller than $p$, Burkhardt (1997) showed that DNA extension can be described as:

$$R_{Odijk} = L\left[1-\alpha_{\square}\left[\left(\frac{h}{p}\right)^{2/3}+\left(\frac{d}{p}\right)^{(2/3)}\right]\right]. \quad (10)$$

The constant $\alpha_{\square}$ has been evaluated by different approaches (Ubbink and Odijk, 1999; Yang *et al.*, 2007), and the most accurate value available is $0.09137 \pm 0.00007$ (Yang *et al.*, 2007). With the known prefactors, Eqs. (9) and (10) are able to give exact predictions of DNA extension, while blob theory only yields scaling predictions.

The hydrodynamic drag acting on this deflection chain can be estimated to be $\zeta \sim 2\pi\eta L/\log(h/d_h)$(Reisner *et al.*, 2005; Batchelor, 1967) with $d_h$ as the hydrodynamic diameter of the chain. This expression represents the drag coefficient of a rod with hydrodynamic interactions screened at the length scale $h$. Neglecting the weak dependence from $\log(h/d_h)$ term, the drag coefficient of the chain $\zeta_{chain} \sim \eta L$, and the diffusivity is:

$$D \sim \zeta^{-1} \sim \eta^{-1} L^{-1}. \quad (11)$$

The relaxation time of the chain is proportional to the ratio of the chain drag coefficient to its spring constant. Given that the free energy of the chain is $F_{Odijk} \approx k_B T \frac{L}{\lambda}$, one finds the spring constant of a deflection chain to be $k_{Odijk} = \frac{\partial^2 F_{Odijk}}{\partial R_{Odijk}^2} \approx L^{-1} h^{-2} p$. Therefore, the predicted scaling of relaxation time is (Reisner *et al.*, 2005):

$$\tau_{Odijk} = \frac{\zeta}{k_{Odijk}} \sim \eta L^2 h^2 p^{-1}. \quad (12)$$

Note that the excluded volume (or $w$) which plays a dominant rule in blob theory does not appear here because it is essentially irrelevant at the length scale of $\lambda << p$.

### 3.3. Polymer in 2D

The configuration of a self-avoiding polymer chain in 2-dimensions has been predicted by Flory theory (Des Cloizeaux and Jannink, 1990; Maier and Rädler, 2000):

$$R_{2D} \sim v_{2D}^{\frac{1}{4}} p^{\frac{1}{2}} N^{\frac{3}{4}} \sim p^{\frac{1}{4}} L^{\frac{3}{4}}. \quad (13)$$

where $v_{2D} \approx p^2$ is the excluded area of a statistical segment. The Flory exponent in 2D (=3/4) turns out exactly the same as obtained using renormalization theory (Des Cloizeaux and Jannink, 1990). To estimate the diffusivity of a chain in a liquid sheet with hydrodynamic interactions, one immediately faces Stokes Paradox (Maier and Rädler, 1999; Leal, 1992). However, confining polymers in 2D can only be achieved in reality by absorbing them on a solid substrate or a lipid membrane. Under such conditions, hydrodynamic interactions are screened and the confined polymers are expected to be Rouse-like (Maier and Rädler, 1999). Consequently, the scalings of diffusivity and relaxation time can be obtained:

$$D_{2D} \sim L^{-1} \quad (14)$$

$$\tau_{2D} \sim R_{2D}^2 / D_{2D} \sim p^{\frac{1}{2}} L^{\frac{5}{2}}. \quad (15)$$

## 4. Experimental techniques

### 4.1. DNA visualization and general experimental setup

The majority of single-molecule experiments employ fluorescence microscopy and enhanced CCD cameras to capture real-time images of stained DNA. Atomic Force Microscopy (AFM) has also been used in a few studies (Rivetti *et al.*, 1996). Commonly used DNA include $\lambda$-DNA (48.5 kbp, $L = 16.3$ μm, $R_g \approx 0.7$ μm), T4-DNA (165.6 kbp, $L = 55.6$ μm, $R_{g,bulk} \approx 1.5$ μm), $\lambda$-DNA concatemers, and restriction enzyme digested $\lambda$-DNA fragments.

DNA are usually stained with intercalating dyes YOYO-1 and TOTO-1 at a base pair to dye ratio ranging from 4 to 10. This intercalation distorts the local DNA structure, and affects DNA contour length and persistence length ($p \approx$ 50 nm for unstained DNA at standard buffer concentrations). For stained λ-DNA at a base pair to dye ratio of 4 : 1, the contour length increases from 16.3 μm to 21~22 μm (Perkins *et al.*, 1995), representing a 29% to 35% increase. However, a careful measurement to determine the influence of dye to DNA persistence length is still lacking.

The experiments were typically performed in a buffer of Tris-EDTA (TE) or Tris-Borate-EDTA (TBE) with pH around 8 to keep DNA properties constant. To prolong the observation time, 0.5 to 4% (v/v) of beta-mercaptoethanol (BME) is typically included in buffers to remove free radicals. In addition to BME, an oxygen scavenger system consisting of glucose oxidase, glucose, and catalase is usually used in studies investigating the dynamics of DNA to further extend the observation time. The benefits brought by these agents are obvious, while the side effects are not fully appreciated. We remark that BME is a weak acid (pKa= 9.6), and the oxygen scavenger system produces gluconic acid (pKa=3.6) as a final product. Both lower the system pH and increase system ionic strength, but the later will lead to an accumulated change with time. Both effects are negligible at moderate buffer concentrations and in typical time course of experiments, but they can have significant influence in low concentration buffers such as those more dilute than 0.05 × TBE or 0.2 × TE (Hsieh *et al.*, 2008).

In many experiments where DNA are driven electrokinetically, it is necessary to treat the channel surface to minimize electroosmotic flow. A commonly used method is dynamic coating with POP-6 (a low molecular weight poly-dimethylacrylamide, a trademark of Applied Biosystems) or low molecular weight poly (n-vinylpyrrolidone) (PVP). Such polar molecules are proposed to absorb on the surface of devices and increase the local viscosity to reduce electroosmotic flow.

Given the $R_{g,bulk}$ of commonly used DNA is around 1 μm, nanoscale devices are often the only choice to serve as the confinement. These devices are typically made by fused silica/Pyrex glass bonded to fused silica/Pyrex/silicon. PDMS has also been successfully used to create nanoscale channels (Jo *et al.*, 2007; Huh *et al.*, 2007), though care must be taken to quench the permeation driven flow (Randall and Doyle, 2005b). Thorough reviews of various fabrication process and design considerations can be found elsewhere in Tegenfeldt *et al.* (2004b) and Douville *et al.* (2008). Fig. 2(a) and 2(b) show typical structures of nanochannels providing tube-like and slit-like confinement.

## 4.2. Transport coefficient analysis

Most experimental studies have investigated confined DNA dynamics at equilibrium, and therefore experimental analysis has focused on extracting DNA diffusivity, relaxation time, and equilibrium size from time-sequence images. To summarize how this is done, we first give a tutorial for analyzing images of confined DNA in slit-like or surface confinement, and briefly address what needs to be changed for chains confined in tube-like confinement.

We define the total fluorescent intensity ($I_0$) and the center of the mass vector ($\mathbf{r}_{cm}$) of a DNA molecule in an image taken at time $t$ as:

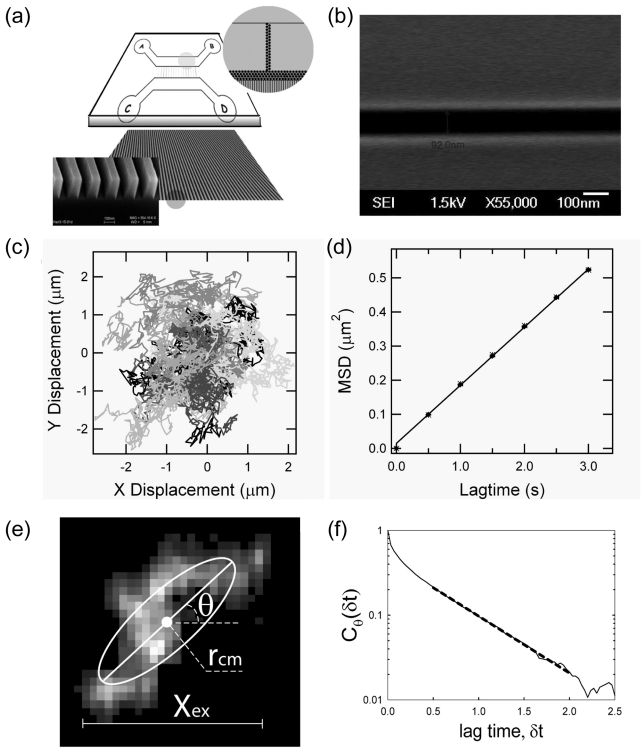


**Fig. 2.** Examples of nanofabricated devices and experimental analysis. Shown in (a) and (b) are images of nanochannels and nanoslits, respectively. (c) Center of mass trajectories for 28 2λ-DNA in a 545 nm tall nanoslit. (d) A representative plot of mean-squared displacement of the center of mass of DNA as a function of lagtime. (e) Illustration of the center of the mass, the orientation, and the extension of a DNA. (f) A representative plot of an ensemble-averaged time autocorrelation functions of DNA confined in nanoslits. The solid line represents experimental results, and the dashed line is a single exponential fit to extract the longest relaxation time. a. Reprinted with permission from Tegenfeldt *et al.* Proc. Natl. Acad. Sci., Copyright 2004 National Academy of Sciences, U.S.A. c. and d. Reprinted with permission from Balducci *et al.* Macromol., Copyright 2006 American Chemical Society. f. Reprinted with permission from Hsieh *et al.* Macromol., Copyright 2007 American Chemical Society.

$$I_0(t) = \sum_{m,n} I_{mn}(t) \tag{16}$$

$$r_{cm,i}(t) = \frac{1}{I_0(t)} \sum_{m,n} r_{mn,i}(t) I_{mn}(t) \tag{17}$$

where $I_{mn}$ is the fluorescent intensity of the pixel [m,n], and i and j represent x or y directions that are perpendicular to the smallest dimension of the slit (z direction). Given the trajectory of $r_{cm}$, the in-plane diffusivity ($D$) can be obtained from the mean-square-displacement ($MSD$)(Savin and Doyle, 2005):

$$MSD = \langle \{ r_{cm,x}(t) - r_{cm,x}(t-\delta t) \}^2 + \{ r_{cm,y}(t) - r_{cm,y}(t-\delta t) \}^2 \rangle = 4D\delta t \tag{18}$$

where [ ] denotes the ensemble average, and $\delta t$ is the lag time. Figs. 2(c) and 2(d) show a collection of DNA center of mass trajectories and a representative plot of MSD vs lag time, respectively.

To obtain more information from DNA images, we define the radius of gyration tensor (**G**):

$$G_{ij}(t) = \frac{1}{I_0(t)} \sum_{m,n} (r_{mn,i}(t) - r_{cm,i}(t)) (r_{mn,j}(t) - r_{cm,j}(t)) I_{mn}(t) \ . \tag{19}$$

**G** carries information of the instantaneous size, shape and orientation of the DNA. The radius of gyration ($R_g$) is the square root of the trace of **G**. The eigenvectors of **G** represent the principle and minor axes that describe the temporal orientation of the DNA. More importantly, the longest relaxation time of the DNA can be extracted from the rate of the change of DNA orientation (Maier and Rädler, 1999, 2000). We first calculate the angle between the principle eigenvector and the x-axis ($\theta(t)$, see Fig. 2(e)):

$$\theta(t) = arctan \frac{\lambda(t) - G_{xx}(t)}{G_{xy}(t)}, \quad \frac{\pi}{2} > \theta(t) > -\frac{\pi}{2} \tag{20}$$

where $\lambda(t)$ is the eigenvalue associated with the principle eigenvector. The time autocorrelation function of $\theta(t)$ is defined by (Maier and Rädler, 2000):

$$C_r(\delta t) = \frac{\langle (\theta(t) - \theta_0)(\theta(t-\delta t) - \theta_0) \rangle}{\langle (\theta(t) - \theta_0)^2 \rangle} \sim \exp((-\delta t)/\tau_1) \quad \text{for } \delta t \geq \tau_1 \tag{21}$$

where $\theta_0$ is the equilibrium average of $\theta(t)$, and should be zero. The longest relaxation times of DNA ($\tau_1$) can be extracted from a single exponential fit to the decay of the rotational autocorrelation function (see Fig. 2(f)). Similarly, we can also define the stretch autocorrelation function ($C_s(\delta t)$) by replacing $\theta$ in Eq. (21) with DNA stretch ($X_{ex}$, see Fig. 2(e)) or $R_g$. For DNA confined in tube-like confinement, the relaxation time is typically obtained from the stretch autocorrelation function (Reisner *et al.*, 2005).

The relaxation time of DNA can also be estimated from the rate of relaxation of a strongly perturbed chain. This is done by prestretching a chain by means of either flow or electric field and then stopping the flow to observe the relaxation of the chain. This method has been used in many studies investigating DNA behavior in bulk (Perkins *et al.*, 1994; Balducci *et al.*, 2007). The relaxation time is extracted from:

$$\langle X_{ex}^2 - X_{ex,0}^2 \rangle = A \exp(-t/\tau_1) \ . \tag{22}$$

where $X_{ex,0}$ is the equilibrium value of $X_{ex}$, and A is a free parameter. We refer to this method as relaxation-after-stretching in future sections.

## 5. Progress in experiments

### 5.1. DNA in slit-like confinement

The first observation of DNA dynamics slowing down in confinement was reported by Bakajin *et al.* (1998). In this pioneering study, T4-DNA were hooked on obstacles and stretched electrophoretically in glass slits with heights of 5 μm, 300 nm and 90 nm. Their relaxation was monitored after DNA disengaged from the obstacles, and was found to be slower in shallower channels. The study was also the first experiment to show that hydrodynamic interactions were totally screened for DNA in a 90 nm nanoslit.

Randall and Doyle (2005b; 2006) and Randall (2006) reported relaxation times of λ-, 2λ- and T4-DNA in 2 μm high slits. The relaxation time of confined T4-DNA (with bulk radius of gyration of approximately 1.5 μm) was found to be almost doubled relative to its bulk value.

Balducci *et al.* (2006) and Chen *et al.* (2004) measured the diffusivity of confined DNA in slit-like channels over a wide range of conditions $0.3 < R_{g,bulk}/h < 15$ (see Fig. 3(a) for the collection of their data on a normalized scale). They found that DNA diffusivity varies inversely with molecular weight for $R_{g,bulk}/h > 1$. The results were in agreement with the blob theory prediction and suggested complete screening of hydrodynamic interactions between blobs. Balducci *et al.* (2006) also provided a scaling analysis to explain why the algebraic decay of the far-field hydrodynamic interaction is sufficient to eliminate large-length scale hydrodynamic cooperativity in the dynamics of quasi-two-dimensional polymers in good solvents. The scaling of DNA diffusivity with channel height was also investigated in detail. The dependence of DNA diffusivity was weaker than the blob theory prediction. Although the height of the smallest slit (70 nm) is very close to the persistence length of DNA, no drastic change of DNA behavior was observed.

Hsieh *et al.* (2007) systematically investigated DNA diffusivity and relaxation time as a function of molecular weight and degree of confinement. The length of DNA ranged from 22.5 kbp to 186 kbp, and the slit height

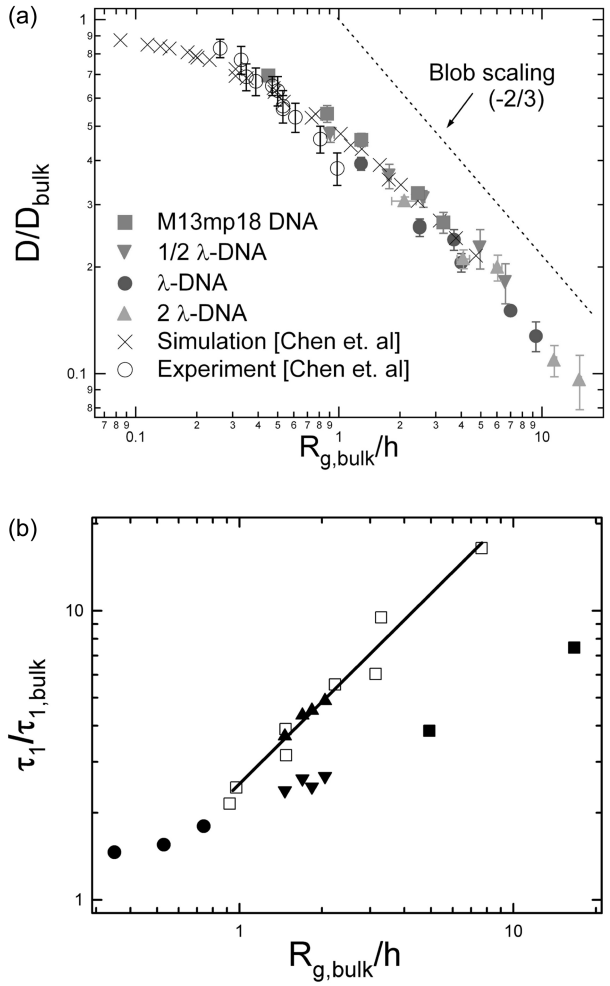


**Fig. 3.** Data for DNA confined in a slit (a) Diffusivity for various DNA molecules and channel heights plotted on normalized axes. Diffusivity is normalized by the bulk diffusivity, and the channel height by the bulk radius of gyration of the DNA. Filled symbols and open circles are experimental data from Balducci *et al.* (2006) and Chen *et al.* (2004), respectively. The × are results from simulations of Chen *et al.* (2004). (b) Collection of DNA relaxation times measured in recent studies. The open squares (□) are those of Hsieh *et al.* (2007) measured from the rotational autocorrelation. The filled symbols represent the relaxation time obtained using relaxation-after-stretching. The circles (●) are from Randall and Doyle (2005a; 2006) and Randall (2006), the squares (■) are from Bakajin *et al.* (1998) and Hsieh *et al.* (2007), and the triangles (▼($\tau_{\rm I}$) and ▲($\tau_{\rm II}$)) are from Balducci *et al.* (2007). The solid line is an empirical fit from Hsieh *et al.* (2007) with slope 0.92. Reproduced with permission from Balducci *et al.* Phys. Rev. Lett., Copyright 2007 American Physical Society.

spanned from 92 nm to 760 nm. It was found $D \sim N^{-0.97\pm0.03} h^{-0.48\pm0.03}$ and $\tau_1 \sim N^{2.45\pm0.04} h^{-0.92\pm0.08}$, in partial agreement with the prediction of blob theory. A cross-examination of experimental results revealed that the origin of the discrepancy is the partial draining nature of "blobs", which leads to a weaker dependence of $\zeta_{chain}$ on $h$. However, the relaxation time measured in this study using the rotational auto-correlation function was much higher than those inferred from the data of Bakajin *et al.* measured using the method of relaxation-after-stretching.

This mystery was resolved by Balducci *et al.* (2007) who studied the relaxation of initially stretched DNA in the linear force-extension regime. Unlike a chain in bulk solutions, a confined chain was found to have two distinct slow relaxation regimes governed by different relaxation times. The crossover extension between the two regimes was found to be in quantitative agreement with the extension of a blob chain with all blobs aligned with the original stretched direction of DNA. $\tau_{\rm I}$ and $\tau_{\rm II}$ denote the time constants controlling the rate of relaxation above and below the crossover extension. Only $\tau_{\rm II}$ agreed with those reported by Hsieh *et al.* (2007), while $\tau_{\rm I}$ and the DNA relaxation times from Bakajin *et al.* (1998) seemed to follow another distinct scaling.

Lin *et al.* (2007) performed experiments and analysis very similar to those of Hsieh *et al.* in nanoslits with $h = 110$ nm, and reported $R_g \sim N^{0.68}$, $D \sim N^{-1.05\pm0.05}$ and $\tau_r \sim N^{2.2}$. Although the scalings reported are close to those found by Hsieh *et al.* (2007), the absolute values of DNA relaxation time in the similar size of nanoslits are very different. The cause of this discrepancy is yet to be determined, but may be due to artifacts produced by DNA photobleaching.

The confined DNA relaxation times reported (and inferred) in the above studies are summarized in Fig. 3(b) and presented as a masterplot of $\tau_1/\tau_{1,bulk}$ versus degree of confinement $R_{g,bulk}/h$. The bulk relaxation time $\tau_{1,bulk}$ and the radius of gyration $R_{g,bulk}$ are estimated using $\tau_{1,bulk} = 0.1\,\eta_s (M/M_{\lambda\text{-}DNA})^{1.8}$ *sec*, and $R_{g,bulk} = 0.7 (M/M_{\lambda\text{-}DNA})^{0.6}$ μm.

Recently, Krishnan *et al.* (2007) reported that DNA was spontaneously localized and extended along the side walls of silicon/Pyrex nanoslits with $h \leq 100$ nm. The relative extension of DNA was fairly independent of h, but was sensitive to the ionic environment (nearly 100% extension at low ionic strength condition). They argued that this phenomenon may be caused by the high curvature at the side walls and did not provide a physical model to further support the argument. Since this is not a universal phenomenon observed in other experiments under similar conditions, the observation might be due to the specific experimental condition and surface treatment of Krishnan *et al.* (2007).

### 5.2. DNA in tube-like confinement

Guo *et al.* (2004) first quantitatively reported that DNA were naturally extended in nanochannels at equilibrium. Although they showed that DNA extension increases with

the decreasing channel size, no comparison was made with existing theories. The study of Tegenfeldt *et al.* (2004a) systemically investigated the extension of confined λ-DNA concatemers in 100 nm × 200 nm nanochannels, and showed that DNA extension scales linearly with its contour length, in agreement with the prediction of blob theory.

Reisner *et al.* (2005) measured λ-DNA extension and relaxation time in nanochannels with dimensions ranging from 440 nm × 440 nm to 30 nm × 40 nm. Their results are shown in Fig. 4. The relaxation time was determined from the stretch autocorrelation function. A distinct change in scalings of DNA extension and relaxation time vs channel height were observed around $h \approx 100$ nm, or about 2 times the DNA persistence length. For $h < 100$ nm, the experimental scalings of DNA extension and relaxation times on channel height were found to be in good agreement with Odijk's predictions (Ubbink and Odijk, 1999). However, for $h \leq 100$ nm it was found $R_{tube} \sim h^{-0.85 \pm 0.05}$ and $\tau_{tube} \sim h^{-0.9 \pm 0.4}$, somewhat deviating from the blob theory predictions of $R \sim h^{-2/3}$(Eq. 3) and $\tau \sim h^{-1/3}$(Eq. 8). Although the deviation is small, it might imply more serious problem because the measured $\tau_{tube}$ showed a stronger $h$ dependence than predicted. This is different from that found in nanoslits where $\tau_{slit}$ depends more weakly on $h$ than predicted due to a stronger screening of hydrodynamic interactions than assumed by blob theory. However, without other information such as DNA diffusivity, it is impossible to draw more firm conclusions.

In the study of entropic recoil of DNA, Mannion *et al.* (2006) reported a single data T4 DNA relaxation time in a 100 nm ± 90 nm nanochannel to be about 4.7 sec. Since it was obtained using the relaxation-after-stretching method, it is likely to be analogous to the $\tau_1$ found by Balducci *et al.* (2007) for DNA confined in a nanoslit.

### 5.3. DNA confined on a surface

Rivetti *et al.* (1996) used AFM to investigate conformation of DNA deposited on mica with different surface treatment. DNA can be either dynamically absorbed or kinetically trapped on the surface. The former will adopt the conformation of a 2D polymer and can diuse and relax, but the latter was fixed on the surface as a projection of the polymer conformation in 3D. The conformation of fully equilibrated DNA with $L < 917$ nm (2712 bp) followed the prediction of a 2D worm-like chain model, while the excluded volume effect becomes important for longer DNA.

Maier and Rädler in a series of three articles (Maier and Rädler, 1999; 2000; 2001) investigated in detail the conformation and dynamics of DNA confined on the surface of a cationic lipid bilayer. They reported $D \sim N^{-0.95 \pm 0.6}$ (for DNA with 40 to 48500 bp) and $R_g \sim N^{0.79 \pm 0.04}$(for DNA with 6141 to 48500 bp). The former suggested a full screening of hydrodynamic interactions, and the latter manifests a self-avoiding walk of DNA in 2D. Consistent with these findings, it was also found $\tau_1 \sim N^{2.6 \pm 0.4}$. The anisotropy of DNA, characterized by the eigenvalues of the radius of gyration tensor, were in excellent agreement with Monte Carlo simulation predictions. The drastic change of DNA properties from 3D to 2D is vividly illustrated by the representative images of λ-DNA in Fig. 1 where both DNA size and anisotropy were shown to greatly increase.

### 5.4. Ionic effects on confined DNA

Ionic environment has been known to have strong influence on biomolecule properties and can be readily manipulated in experiments. However, the combined effects of confinement and ionic environment on polyelectrolytes, critical for many applications, are yet to be fully understood.

For polyelectrolytes, Coulomb interactions introduce a new length scale (Debye screening length, $\kappa^{-1}$) to the molecule, and give rise to both local and non-local effects

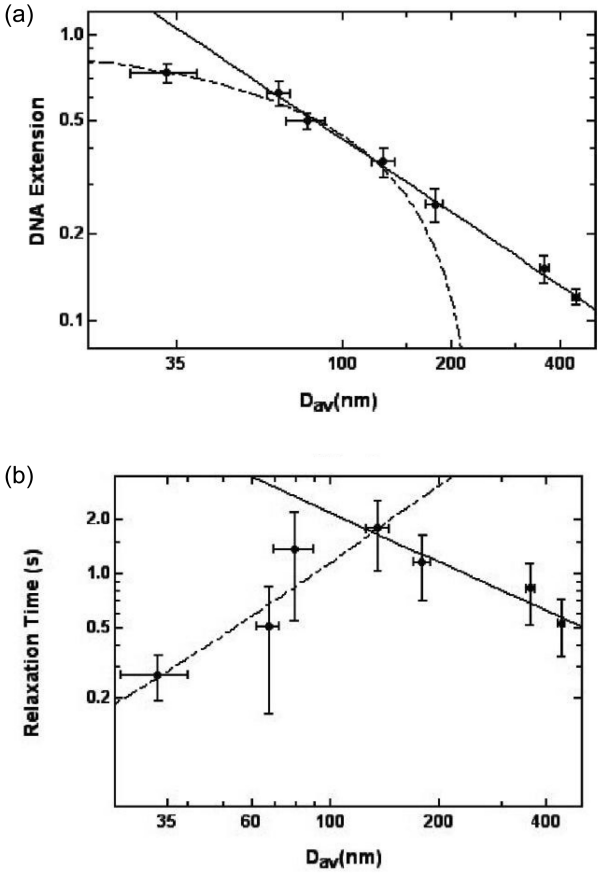


**Fig. 4.** DNA confined in a tube-like geometry. (a) Normalized λ-DNA extension and (b) the longest relaxation time as a function of $D_{av}$, the geometric average of the channel depth and height. The bold lines are best power-law fits. The dashed lines are the fits to the Odijk prediction. Reprinted with permission from Reisner *et al.* Phys. Rev. Lett., Copyright 2005 American Physical Society.

(Odijk and Houwaart, 1978). The former results in an increase of chain stiffness, and the latter resembles an excluded volume between chain segments. A polyelectrolyte can be considered as a neutral polymer with its $p$ and $w$ having an electrostatic contribution depending on ionic environment (Odijk and Houwaart, 1978; Fixman and Skolnick, 1978). This concept has been adopted in recent studies to explain the ionic effects on confined DNA (Jo *et al.*, 2007; Reisner *et al.*, 2007; Hsieh *et al.*, 2008).

To use the above approach, it is necessary to understand the ionic effects on $p$ and $w$. A theoretical prediction of the electrostatically mediated effective diameter of DNA has been given by Stigter (1977). He estimated $w$ of DNA molecules by matching the second virial coefficient of a dilute solution containing charged rods with finite ionic strength to that of the same solution containing neutral rods with a known diameter. The estimated effective diameter of DNA is a function of the line charge, the intrinsic diameter and ionic strength, and was calculated numerically by Poisson-Boltzmann equation. The prediction of w has been shown adequate to quantitatively describe DNA conformational properties (Shaw and Wang, 1993; Rybenkov *et al.*, 1993; Vologodskii and Cozzarelli, 1995).

On the other hand, the ionic effects on DNA persistence length is still an issue under debate (Dobrynin and Rubinstein, 2005). The most well known prediction of DNA persistence length at different ionic strength ($I$) was given by theory of Odijk (1977), and Skolnick and Fixman (1977) (OSF):

$$p = p_0 + p_{el} = p_0 + \frac{0.0324M}{I} nm \tag{23}$$

where $p_0$ is the intrinsic persistence length and $p_{el}$ is the electrostatic persistence length. The most significant prediction of OSF theory was $p_{el} \sim \kappa^{-2}$. Baumann *et al.* (1997) has shown experimentally that the measured electrostatic persistence length agrees with the OSF prediction.

However, OSF theory has been challenged by several experimental studies that reported $p_{el} \sim \kappa^{-1}$ for semiflexible polymers (including DNA). Recently, Dobrynin and Rubinstein 2005; 2005 pointed out that OSF theory was incorrect because the torsional angle between successive bonds was implicitly fixed in the derivation. If this constraint is removed, $p_{el} \sim \kappa^{-1}$ is obtained. Dobrynin (2006) provided an empirical formula of the electrostatic persistence length of DNA:

$$p = p_0 + p_{el} = 46.1 + \frac{1.9195M}{\sqrt{I}} nm \tag{24}$$

Although the persistence lengths given by OSF theory and the empirical fitting follow distinct scalings at very low ionic strength, they are similar and depend very weakly on $I$ for $I > 1$ mM. On the other hand, the effective diameter of DNA depends strongly on $I$ even at $I \approx 0.5$M. Therefore, it is expected that the ionic effects on DNA will be dominated by the change in the effective diameter for $0.5\text{M} > I > 1$ mM.

Jo *et al.* (2007) and Reisner *et al.* (2007) investigated the ionic effects on DNA extension in tube-like confinement. The former was performed in 100 nm × 1000 nm PDMS channels with buffers successively diluted from 1 × TE (reported $I = 8.4$ mM). The ionic strength was assumed to be inversely proportional to the degree of dilution. The relative extension of T4 and λ-DNA was very close to each other and increased with decreasing TE buffer concentration, and seemed to approach a plateau of 60% extension for $I < 0.05 \times$ TE. The prediction of Eq. (10) with $p$ evaluated using Eq. (23) was compared with the data, implying that the chain was in Odijk's deflection chain regime. The predicted DNA extension agreed well with the measured for $I > 0.05 \times$ TE, but was overestimated at lower $I$. It is surprising that DNA extends more than 50% at $I \approx 0.4$mM (or $p \approx 131\ nm$ using Eq. (23)) because the channel width (1000 nm) is much larger than the persistence length. However, Jo *et al.* (2007) argued that such an unexpected high extension of DNA is because an entropic penalty prevents DNA to form "hairpins" (Odijk, 2006).

In the study of Reisner *et al.* (2007), ionic effects on λ-DNA extension were studied in near-square glass nanochannels with dimensions of roughly 50 nm, 100 nm, and 200 nm. The ionic strength was tuned in the range of 4 mM to 300 mM by varying TBE buffer concentration. They found in all three sizes of nanochannels that DNA extended more with lower ionic strength. Moreover, the degree of change of DNA extension were in good agreement with predicted scaling given by Eq. (3) with $p$ and $w$ described by OSF theory (Eq. (23)) and Stigter's estimation (Stigter, 1977). We note that although their own earlier study (Reisner *et al.*, 2005) showed a moderate deviation between blob theory and measured DNA extension, Eq. (3) with predicted exponents was used without modication. Most surprisingly, the prediction given by deflection chain theory that was employed by Jo *et al.* (2007) was not even qualitatively similar to the trend observed in this study.

A very recent work of Zhang *et al.* (2008) reported extension of T4-DNA confined in rectangular PDMS channels with a depth of 300 nm and a width in the range from 150 to 300 nm. The buffer ionic strength was varied between 35 mM and 0.3 mM. The increase of DNA extension with decreasing $I$ was again explained by blob theory. However, the authors have estimated the excluded volume parameter $z$ of a blob (Yamakawa, 1967) and found that $z$ is too small for a blob to follow the long chain scaling of $g \sim h^{\frac{5}{3}} w^{-\frac{1}{3}} p^{-\frac{4}{3}}$. As a result, the authors chose to use a perturbation expansion to estimate the coil swelling factor of a blob (Yamakawa, 1967) and therefore $N_b$ in a chain. In the calculation of $z$, $p$ and $w$ were also estimated by OSF

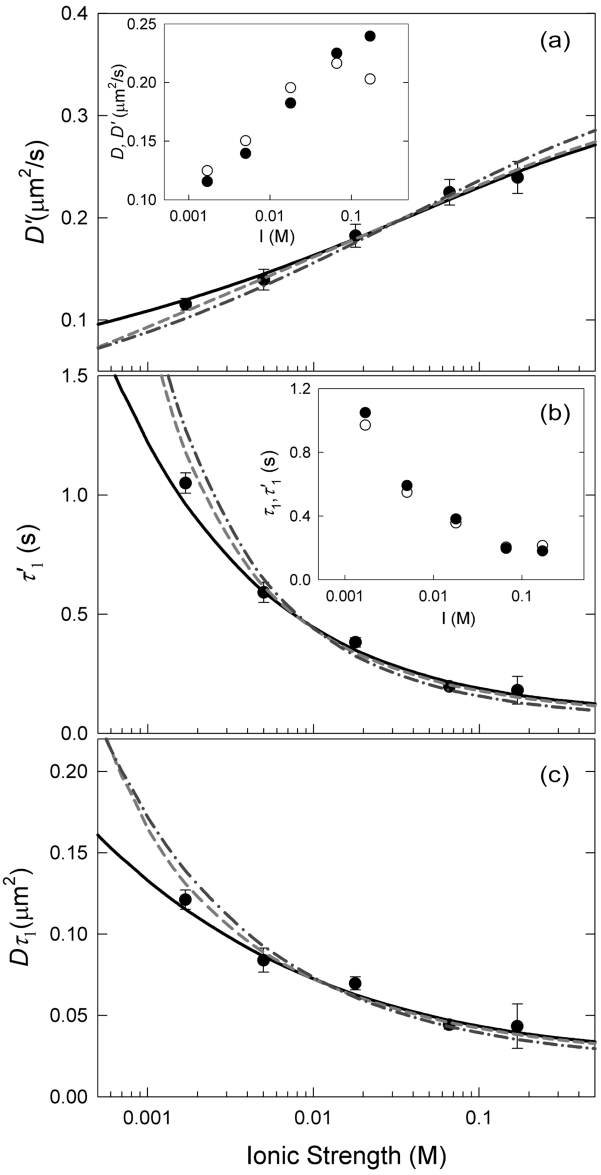


**Fig. 5.** λ-DNA (a) diffusivity, (b) relaxation time, and (c) size as functions of ionic strength. Eqs. (5), (6) and (2) are fit to DNA diffusivity, relaxation time and size, respectively. The solid, dashed and dashed-dotted curves are the fittings with $p$ described as a constant, by Eq. (23), and by Eq. (24), respectively. $w$ is estimated using Stigter's prediction (Stigter, 1977) for all fittings. Only the four data points at highest ionic strength were used in the fittings so that the relatively weak contribution to DNA properties from the change of $p$ can be distinguished at the lowest ionic strength. The insets in (a) and (b): The measured diffusivity and longest relaxation time before (open symbols) and after (filled symbols) viscosity adjustment. A scaled diffusivity $D'=(D\eta/\eta_{ref})$ and a scaled relaxation time $\tau_1'=(\tau_1\eta_{ref}/\eta)$ were defined to remove viscosity effects from the data. The reference viscosity ($\eta_{ref}$) is taken to be 1 cp. Reprinted with permission from Hsieh *et al.* (2008) Nano Lett., Copyright 2008 American Chemical Society.

theory (Eq. (23)) and Stigter's estimation (Stigter, 1977). It was concluded that the elongation of the DNA molecules with decreasing ionic strength is mainly caused by the increase of the persistence length while the excluded volume effect plays a very minor role due to the relatively small number of statistical segments within each blob.

The above experiments were performed in a regime where $p \approx h$, and as a result it can be confusing whether blob theory or deflection chain theory or neither is appropriate to describe DNA behavior. Furthermore, only DNA conformation was investigated but ionic effects on DNA dynamics is yet to be studied. To address these issues, Hsieh *et al.* (2008) chose to perform experiments to examine the ionic effects on λ-DNA in 450 nm high glass nanoslits. The diffusivity, relaxation time and conformation were measured at $I$=1.7 –170 mM. In this study, the ionic contribution of each added chemicals were carefully evaluated, and oxygen was blocked from the experimental platform to reach a more stringent control of system ionic strength. Fig. 5 shows a good agreement between experimental results and the proportionality fittings to the blob theory prediction with an electrostatically mediated effective width and persistence length. Although it was not clear whether Eq. (23) or Eq. (24) is more accurate from the experimental results, it did suggest that the effective diameter of DNA, representing the electrostatic repulsion between remote DNA segments, is the main driving force for the observed change in DNA properties at these physiological ionic strengths.

To finish this section we remark that the interplay between the ionic environment and the negatively charged glass channel can induce additional effects on DNA. For example, as a channel becomes smaller or ionic strength becomes lower so that $h\kappa \approx O(1)$, one will expect a reduction in the effective dimension of the confinement due to the co-ion depletion near the boundary. Also at the same limit, electroneutrality will lead to an enrichment of the counterions in nanochannels, and charge regulation could occur on the surfaces of DNA and the channel (Israelachvili, 1991). These phenomena can cause opposite effects on DNA behavior, and can be difficult to isolate.

### 5.5. Confinement-induced entropic recoil force

Recently, Craighead and coworkers electrophoretically drove DNA from a microchannel into a nanochannel and observed that DNA recoils (retreat) if it is only partially inserted into the nanochannel (Cabodi *et al.*, 2002; Turner *et al.*, 2002; Craighead, 2006; Mannion *et al.*, 2006). This recoil process is driven by the entropy difference between DNA segments inside and outside of confinement, which is qualitatively different from the entropic elastic force that causes a stretched chain to relax. The latter is driven by the entropic difference of DNA between a stretched state and equilibrium. Fig. 6 illustrates the different outcomes when

these two entropic forces acting on confined DNA. The relaxation of a stretched DNA is fastest in the beginning and becomes slower when DNA approaches equilibrium due to the depletion of the entropy difference (see Fig. 6(a) and (b)). On the contrary, the DNA recoil speeds up over time because entropic recoil force is constant while the drag acting on confined DNA is diminishing (see Fig. 6(a) and (c)). The DNA extension during the relaxation and recoil processes can be described as (Turner *et al.*, 2002; Mannion *et al.*, 2006):

$$l(t) = l_0 + (l_E - l_0)\exp((-t)/\tau) \tag{25}$$

$$l_I(t) = \sqrt{-(f/\rho)(t - t_0)}\,. \tag{26}$$

where $l(t)$ is the length of a stretched chain in confinement, $l_0$ is the equilibrium length of the chain when it is fully confined, $l_E$ is the initial length of DNA before relaxation, $\tau$ is the relaxation time, $l_I(t)$ is the length of a partially confined chain, $f$ is the entropic recoil force, $\rho$ is the drag per unit $l_I(t)$, and $t_0$ is the time when the recoil process ends. Note that Eq. (25) is a variation of Eq. (22). Although both formulas can describe the relaxation of a stretched chain, the relaxation time obtained from the former will be about two times of that from the latter. If DNA is partially stuck at the entrance of a nanochannel while the part in the nanochannel is stretched, a combined relaxation and recoil process can happen when the electric field that drives DNA stops (see Fig. 6(a) and (d)). The length of such a chain can be described by (Mannion *et al.*, 2006):

$$l_{I,e}(t) = [(l(t)/l_0)]\,l_I(t) \tag{27}$$

By fitting the DNA extension during recoil to Eq. (26), one can obtain the value of $f/\rho$. Using $\rho$ inferred from electrophoretic mobility of confined DNA, Craighead and coworkers (Turner *et al.*, 2002; Mannion *et al.*, 2006) estimated the entropic recoil force $f$ and found that it was at the same order of magnitude as that inferred from relevant theories (Mannion *et al.*, 2006).

### 5.6. Confined DNA in pressure-driven flow

The behavior of confined DNA in pressure-driven flow has been studied by Stein *et al.* (2006) in slit-like channels with $h = 175$ nm to 3.8 μm. For weakly confined DNA with $R_g/h < 0.3$, the pressure-driven mobility was found to increase with molecular weight due to the mechanism of hydrodynamic chromatography-larger DNA are sterically confined to the center of the slit and on average sample a faster velocity. On the other hand, the mobility of strongly confined chains ($R_g/h > 1$) became independent of molecular weight due to a constant segment distribution profile over the channel height, regardless of the size of DNA. The Taylor dispersion of DNA molecules was highly suppressed in confined channels and decayed with decreasing channel height and increasing molecular length.

Another unique phenomenon (Stein *et al.*, 2006; Larson *et al.*, 2006) of confined DNA in pressure-driven flow is that DNA were not deformed even at high Weissenberg number ($Wi$) defined by $Wi = \tau_1\dot{\gamma}$. Here $\dot{\gamma}$ is the velocity gradient in the smallest dimension of the geometry. In bulk, DNA starts to extend at $Wi \geq 1$. The reason behind this anomaly is that the flow gradient is applied over only a

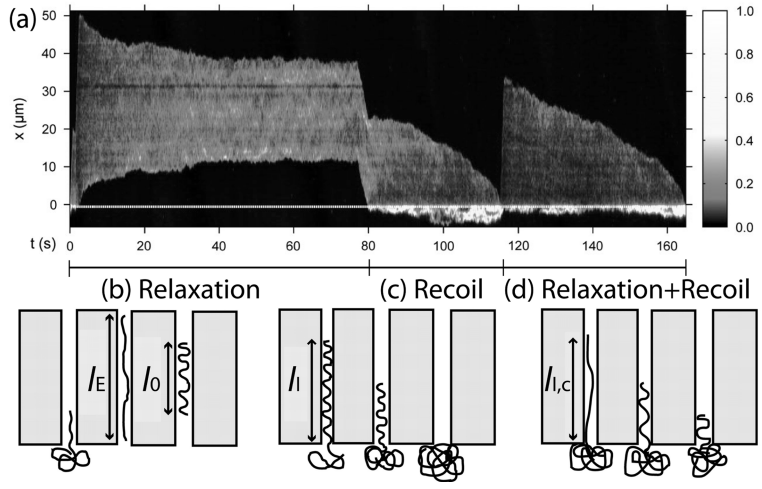


**Fig. 6.** Experimental images and schematic of DNA contraction, recoil and a combined process of the two in confinement. (a) Normalized intensity of a single T4 DNA along the channel ($x$ axis) versus time $t$. At $t = 0$ the molecule is stretched while being driven electrophoretically from the microchannel ($x \leq 0$) into the nanochannel ($x > 0$). The DNA stays in the nanochannel and contracts until reaching equilibrium (illustrated in (b)). At $t = 77$ s, the DNA is moved to the nanochannel entrance by a weak pulse field. Since a small part of DNA straddles the interface, the molecule begins to recoil from the nanochannel into the microchannel (illustrated in (c)). At $t = 115$ s, DNA is driven partially into channel with a strong pulse. When the field is turned o, DNA begins to both contract and recoil simultaneously (illustrated in (d)). Reprinted with permission from Mannion *et al.* Biophys. J., Copyright 2006 the Biophysical Society.

blob and not the whole chain. Since a blob is only a fraction of the molecule, the relevant Weissenberg number $Wi = \tau_{blob}\dot{\gamma}$ is usually well below 1, and leads to no DNA deformation (Hsieh *et al.*, 2007). This picture is applicable to DNA in nanoslits and nanochannels with constant dimensions. Due to this limitation, one usually deforms confined DNA by an induced extensional flow generated by changing the width of the confinement. Since the width of a slit is much larger than a DNA molecule, the flow gradient applies over the whole chain and DNA can be easily stretched. Therefore, a nanoslit with a cross-slot or a contraction (Chan *et al.*, 2004; Larson *et al.*, 2006) is the choice for stretching confined DNA with pressure-driven flow.

Finally, a feature that was understood by simulations (Jendrejack *et al.*, 2003a,b) but so far only been observed for weakly confined DNA in microchannels (Chen *et al.*, 2005; Fang *et al.*, 2007) is a shear-induced migration from the boundary. It is a consequence of shear-induced DNA stretch combined with boundary-mediated hydrodynamic interactions. We note that pressure-driven flow has not been the dominant mechanism used in nano-scale confinement to drive DNA because a large pressure is needed to generate a sufficiently large flow in such small dimensions.

### 5.7. Electrokinetically driven DNA in confinement

DNA as a polyelectrolyte can be easily manipulated by applying electric fields. The most common electrokinetic mechanism used in single-molecule DNA studies is electrophoresis. However, most channels have charged surfaces and thus a background electroosmotic flow is also present, unless special surface treatment has been done to suppress electroomosis.

The first studies of DNA electrophoresis in well-defined nano-confinement were performed by Austin and coworkers (Volkmuth and Austin, 1992; Volkmuth *et al.*, 1994). The experiments were carried out in 150 nm deep nanoslits with cylindrical obstacles to mimic the structure of agarose gel for DNA separation. DNA used in these studies had contour lengths of 5-30 μm and were confined in the nanoslits. DNA mobility was found to be independent of its contour length if no collisions occured (Volkmuth *et al.*, 1994), as is found for unconfined DNA. However, once DNA collide and hook on obstacles, the average time required for DNA to unhook depends on their size. Consequently, the mobility of DNA passing through the obstacle array becomes length dependent. Following this pioneering work, many studies have been done to further understand the collision and unhooking processes in microchannels with obstacles (Randall and Doyle, 2004; 2005a; Teclemariam *et al.*, 2007) while no research has been done to investigate what effects confinement brings to this process.

Recently, several groups have reported that confinement alone can result in a length-dependent electrokinetic DNA mobility. Campbell *et al.* (2004) reported a systematic measurement of λ-DNA mobility in tube-like nanochannels with dimensions from 870 nm × 730 nm to 150 nm × 180 nm. No agent was used to suppress the electroosmotic flow and therefore the measured DNA mobility was a sum of electrophoresis and electroosmosis. The DNA mobility was found to increase with decreasing channel size. This observation was qualitatively explained as a result of weakening electroosmotic flow in shallower channels due to the increasing overlapping of the wall potential. Cross *et al.* (2007) observed that DNA mobility decreases with molecular weight in 19 nm deep nanoslits while the same phenomenon was not seen in 70 nm nanoslits. The electroosmotic flow was suppressed by dynamic coating using the polymer PVP, and the operating electric field was only up to 125 V/cm. DNA size used is between 2 to 10 kbp. The mobility scaled as $L^{-\frac{1}{2}}$, in excellent agreement with a model proposed using blob theory and the assumption that the friction between DNA and the boundary is proportional to their contact area. However, we note that blob theory may not be the appropriate model to describe DNA configuration in such a small geometry. On the other hand, a very recent study of Salieb-Beugelaar *et al.* (2008) has reported a field-dependent DNA electrophoretic mobility measured in 20 nm deep nanoslits. The experiments were performed at fields of 60-2000 *V*/cm, much stronger than those used in Cross *et al.* (2007). The overall DNA electrophoretic mobility was found to increase for 60 $V$/cm $\leq E \leq$ 300 $V$/cm and to decrease for $E \geq$ 300 $V$/cm. The rise of DNA electrophoretic mobility at moderate fields was not explained, but the decrease of DNA electrophoretic mobility at high fields was explained as a result of dielectrophoretic DNA trapping due to the surface roughness (Salieb-Beugelaar *et al.*, 2008). Although the above studies suggest that a length-dependent or field-dependent DNA mobility may be achievable using confinement alone, available experimental results are too scarce and need to be reproduced to confirm their universality.

Quantitative study of electrophoretic stretching confined DNA was first performed by Bakajin *et al.* (1998) using silt-like channels with obstacles. The experimental results showed negligible intramolecular hydrodynamic interactions in the smallest channel used (90 nm), and also supported the notion of electro-hydrodynamic equivalence (Long *et al.*, 1996). Since then, several groups have studied DNA stretching in microchannels (Ferree and Blanch, 2003; Randall and Doyle, 2004; Juang *et al.*, 2004; Randall and Doyle, 2005a; 2006; Randall *et al.*, 2006), however the DNA was not confined. In a recent demonstration to stretch DNA in a 2 μm high T-shape channel using electric field gradients, Tang and Doyle (2007) showed that they

can trap and nearly fully stretch a λ-DNA 10-mer (485 kbp, $L \approx 215$ μm, $R_{g,bulk} \approx 2.8$ μm) (see Fig. 7), which has equilibrium size much larger than the channel height. Therefore, such devices can potentially be the platform for the future studies in field induced stretching and the role of confinement.

Electrophoresis of DNA confined on a surface has been studied by Olson *et al.* (2001) and Maier *et al.* (2002). The former study observed DNA electrophoresis on a lipid bilayer with the presence of obstacles (presumably defects in the bilayer). The unhooking of DNA from obstacles was qualitatively similar to that observed in 3D. In Ref.(Maier *et al.*, 2002), DNA was absorbed on a lipid bilayer with one end tethered to a solid support. DNA was stretched by an electric field, and its extension was found to agree with the prediction given by a 2D worm-like chain model.

## 6. Summary and outlook

Single-molecule experimental studies of confined DNA has expanded our fundamental understanding in polymer physics, and also opened a new field for future applications.

For equilibrium dynamics, we have gained a sound understanding of DNA confined in a slit-like geometry where the influence of degree of confinement, molecular weight and ionic environment on DNA behavior has been characterized. The framework of blob theory was shown to be adequate for describing the observed DNA conformation and dynamics with an expected compromise in the assumption of non-draining blobs. However, a less complete picture for confined DNA in a tube-like geometry has been reached. Measured DNA extension and relaxation time were in moderate agreement with blob theory while the cause of the deviation remains unclear because measurement of DNA diffusivity is lacking in this geometry. Moreover, the experimental results for ionic effects on DNA are inconsistent in different studies. Here more complexity was involved because many experiments were performed at a channel height $h \approx 2p$ where the transition between deflection chain regime and blob theory regime is rather vague and not well understood. A possible remedy would be using actin as the model polymer ($p \approx 16$ μm) and therefore the transition between the two regimes can be readily investigated in microchannels.

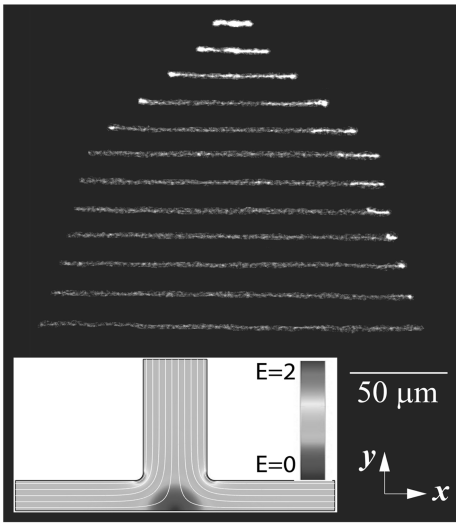


**Fig. 7.** Electrophoretic stretching of a λ-DNA 10-mer in a 2 μm high T channel. Inserted plot shows the dimensionless electric field strength in the T-junction region from finite element calculation. Reprinted with permission from Tang and Doyle App. Phys. Lett., Copyright 2007 American Institute of Physics.

For non-equilibrium dynamics of confined DNA, few quantitative studies have been performed. The relative minor progress in this field is probably hindered by the lack of understanding of the equilibrium state of confined polymers and the expectation that a highly deformed confined DNA will behave qualitatively similar to unconfined DNA except with screened hydrodynamic interactions. However, even if this picture is correct, the very different equilibrium states of unconfined and confined DNA are expected to result in significant difference in, for example, the coil-stretch transition. The very recent reports on confinement and electric field dependent DNA mobility observed in extremely small geometries ($h \approx 20$ nm) highlight the importance of the surface interaction on the transport of confined DNA. It is also likely that the ionic environment in such small channels is different from the bulk condition. As strongly implied by these studies, different surface treatment and the possible interplay between charged DNA and confinement should be considered as important factors in future experimental design and analysis. These are just some of the unanswered questions in this field and show that much exciting research is still left to be performed.

Funding for this work was provided by NSF Career Grant No. CTS-0239012 and U. S. Genomics.

## References

Bakajin, O. B., T. A. J. Duke, C. F. Chou, S. S. Chan, R. H. Austin and E. C. Cox, 1998, Electrohydrodynamic stretching of DNA in confined environments, *Phys. Rev. Lett.* **80**, 2737-2740.

Balducci, A. and C. C. Hsieh, P. S. Doyle, 2007, Relaxation of stretched DNA in slitlike confinement, *Phys. Rev. Lett.* **99**, 4.

Balducci, A., P. Mao, J. Y. Han and P. S. Doyle, 2006, Double-stranded DNA diffusion in slitlike nanochannels, *Macromolecules* **39**, 6273-6281.

Batchelor, G K., 1967, An introduction to fluid dynamics, Cambridge University Press, Cambridge.

Baumann, C. G., S. B. Smith, V. A. Bloomfield and C. Bustamante, 1997, Ionic effects on the elasticity of single DNA molecules, *Proc. Natl. Acad. Sci. USA* **94**, 6185-6190.

Brochard, F., 1977, Dynamics of polymer chains trapped in a slit, *J. Phys. (Paris)* **38**, 1285-1291.

Brochard, F. and P. G. de Gennes, 1977, Dynamics of confined polymer chains, *J. Chem. Phys.* **67**, 52-56.

Burkhardt, T. W., 1995, Free energy of a semiflexible polymer confined along an axis, *J. Phys. A* **28**, L629-L635.

Burkhardt, T. W., 1997, Free energy of a semiflexible polymer in a tube and statistics of a randomlyaccelerated particle, *J. Phys. A* **30**, L167-L172.

Cabodi, M., S. W. P. Turner and H. G. Craighead, 2002, Entropic recoil separation of long DNA molecules, *Anal. Chem.* **74**, 5169-5174.

Campbell, L. C., M. J. Wilkinson, A. Manz, P. Camilleri and C. J. Humphreys, 2004, Electrophoretic manipulation of single molecules in nanofabricated capillaries, *Lab Chip* **4**, 225-229.

Chan, E. Y., N. M. Goncalves, R. A. Haeusler, A. J. Hatch, J. W. Larson, A. M. Maletta, G. R. Yantz, E. D. Carstea, M. Fuchs, G. G. Wong, S. R. Gullans and R. Gilmanshin, 2004, DNA mapping using microfluidic stretching and single-molecule detection of fluorescent site-specific tags, *Genome Res.* **14**, 1137-1146.

Chen, Y. L., M. D. Graham, J. J. de Pablo, K. Jo and D. C. Schwartz, 2005, DNA molecules in microfluidic oscillatory flow, *Macromolecules* **38**, 6680-6687.

Chen, Y. L., M. D. Graham, J. J. de Pablo, G. C. Randall, M. Gupta and P. S. Doyle, 2004, Conformation and dynamics of single DNA molecules in parallel-plate slit microchannels, *Phys. Rev. E* **70**, 060901.

Craighead, H., 2006, Future lab-on-a-chip technologies for interrogating individual molecules, *Nature* **442**, 387-393.

Cross, J. D., E. A. Strychalski and H. G. Craighead, 2007, Size-dependent DNA mobility in nanochannels, *J. Appl. Phys.* **102**, 024701.

Daoud, M. and P. G. de Gennes, 1977, Statistics of macromolecular solutions trapped in small pores, *J. Phys. (Paris)* **38**, 85-93.

de Gennes, P. G., 1976, Dynamics of entangled polymer-solutions 1. rouse model, *Macromolecules* **9**, 587-593.

Dechadilok, P. and W. M. Deen, 2006, Hindrance factors for diffusion and convection in pores, *Ind. Engin. Chem. Res.* **45**, 6953-6959.

Deen, W. M., 1987, Hindered transport of large molecules in liquid-filled pores, *AICHE J.* **33**, 1409-1425.

Des Cloizeaux, J. and G. Jannink, 1990, Polymers in solution : their modelling and structure, Oxford science publications, Oxford University Press, New York.

Dobrynin, A. V., 2005, Electrostatic persistence length of semiflexible and flexible polyelectrolytes, *Macromolecules* **38**, 9304-9314.

Dobrynin, A. V., 2006, Effect of counterion condensation on rigidity of semiflexible polyelectrolytes, *Macromolecules* **39**, 9519-9527.

Dobrynin, A. V. and M. Rubinstein, 2005, Theory of polyelectrolytes in solutions and at surfaces, *Prog. Polym. Sci.* **30**, 1049-1118.

Douville, N., D. Huh and S. Takayama, 2008, DNA linearization through confinement in nanofluidic channels, *Anal. Bioanal. Chem.* **391(7)**, 2395-2409.

Eijkel, J. C. T. and A. van den Berg, 2005, Nanofluidics: what is it and what can we expect from it?, *Microfluidics and Nanofluidics* **1**, 249-267.

Fang, L., C. C. Hsieh and R. G. Larson, 2007, Molecular imaging of shear-induced polymer migration in dilute solutions near a surface, *Macromolecules* **40**, 8490-8499.

Ferree, S. and W. H. Blanch, 2003, Electrokinetic stretching of tethered DNA, *Biophys. J.* **85**, 2539-2546.

Fixman, M. and J. Skolnick, 1978, Polyelectrolyte excluded volume paradox, *Macromolecules* **11**, 863-867.

Gorbunov, A. A. and A. M. Skvortsov, 1995, Statistical properties of confined macromolecules, *Adv. Colloid Interface Sci.* **62**, 31-108.

Guo, L. J., X. Cheng and C. F. Chou, 2004, Fabrication of size-controllable nanofluidic channels by nanoimprinting and its application for DNA stretching, *Nano Lett.* **4**, 69-73.

Han, J. and H. G. Craighead, 2000, Separation of long DNA molecules in a microfabricated entropic trap array, *Science* **288**, 1026-1029.

Han, J., S. W. Turner and H. G. Craighead, 1999, Entropic trapping and escape of long DNA molecules at submicron size constriction, *Phys. Rev. Lett.* **83**, 1688-1691.

Han, J. Y. and H. G. Craighead, 2002, Characterization and optimization of an entropic trap for DNA separation, *Anal. Chem.* **74**, 394-401.

Han, J. Y., J. P. Fu and R. B. Schoch, 2008, Molecular sieving using nanofilters: Past, present and future, *Lab Chip* **8**, 23-33.

Harden, J. L. and M. Doi, 1992, Diffusion of macromolecules in narrow capillaries, *J. Phys. Chem.* **96**, 4046-4052.

Hsieh, C. C., A. Balducci and P. S. Doyle, 2007, An experimental study of DNA rotational relaxation time in nanoslits, *Macromolecules* **40**, 5196-5205.

Hsieh, C. C., A. Balducci and P. S. Doyle, 2008, Ionic effects on the equilibrium dynamics of dna confined in nanoslits, *Nano Lett.* **8**, 1683-1688.

Huh, D., K. L. Mills, X. Y. Zhu, M. A. Burns, M. D. Thouless and S. Takayama, 2007, Tuneable elastomeric nanochannels for nanofluidic manipulation, *Nat. Mater.* **6**, 424-428.

Israelachvili, J. N., 1991, Intermolecular and surface forces, Academic Press, London ; San Diego, 2nd edition.

Jendrejack, R. M., E. T. Dimalanta, D. C. Schwartz, M. D. Graham and J. J. de Pablo, 2003a, DNA dynamics in a microchannel, *Phys. Rev. Lett.* **91**, 038102.

Jendrejack, R. M., D. C. Schwartz, M. D. Graham and J. J. de Pablo, 2003b, Effect of confinement on DNA dynamics in microfluidic devices, *J. Chem. Phys.* **119**, 1165-1173.

Jo, K., D. M. Dhingra, T. Odijk, J. J. de Pablo, M. D. Graham, R. Runnheim, D. Forrest and D. C. Schwartz, 2007, A single-molecule barcoding system using nanoslits for DNA analysis, *Proc. Natl. Acad. Sci. USA* **104**, 2673-2678.

Juang, Y. J., S. Wang, X. Hu and L. J. Lee, 2004, Dynamics of single polymers in a stagnation flow induced by electrokinetics, *Phys. Rev. Lett.* **93**, 268105.

Kasianowicz, J. J., E. Brandin, D. Branton and D. W. Deamer, 1996, Characterization of individual polynucleotide molecules using a membrane channel, *Proc. Natl. Acad. Sci. USA* **93**, 13770-13773.

Krishnan, M., I. Monch and P. Schwille, 2007, Spontaneous stretching of DNA in a two-dimensional nanoslit, *Nano Lett.* **7**, 1270-1275.

Larson, J. W., G. R. Yantz, Q. Zhong, R. Charnas, C. M. D'Antoni, M. V. Gallo, K. A. Gillis, L. A. Neely, K. M. Phillips, G. G. Wong, S. R. Gullans and R. Gilmanshin, 2006, Single DNA molecule stretching in sudden mixed shear and elongational microflows, *Lab Chip* **6**, 1187-1199.

Leal, L. G., 1992, Laminar flow and convective transport processes : scaling principles and asymptotic analysis, Butterworth-Heinemann, Boston.

Lin, P. K., C. C. Fu, Y. L. Chen, Y. R. Chen, P. K. Wei, C. H. Kuan and W. S. Fann, 2007, Static conformation and dynamics of single DNA molecules confined in nanoslits, *Phys. Rev. E* **76**, 011806.

Long, D., J. L. Viovy and A. Ajdari, 1996, Simultaneous action of electric fields and nonelectric forces on a polyelectrolyte: Motion and deformation, *Phys. Rev. Lett.* **76**, 3858-3861.

Lubensky, D. K. and D. R. Nelson, 1999, Driven polymer translocation through a narrow pore, *Biophys. J.* **77**, 1824-1838.

Maier, B. and J. O. Rädler, 1999, Conformation and self-diffusion of single DNA molecules confined to two dimensions, *Phys. Rev. Lett.* **82**, 1911-1914.

Maier, B. and J. O. Rädler, 2000, DNA on fluid membranes: A model polymer in two dimensions, *Macromolecules* **33**, 7185-7194.

Maier, B. and J. O. Rädler, 2001, Shape of self-avoiding walks in two dimensions, *Macromolecules* **34**, 5723-5724.

Maier, B., U. Seifert and J. O. Rädler, 2002, Elastic response of DNA to external electric fields in two dimensions, *Europhys. Letters* **60**, 622-628.

Mannion, J. T. and H. G. Craighead, 2007, Nanofluidic structures for single biomolecule fluorescent detection, *Biopolymers* **85**, 131-143.

Mannion, J. T., C. H. Reccius, J. D. Cross and H. G. Craighead, 2006, Conformational analysis of single DNA molecules undergoing entropically induced motion in nanochannels, *Biophys. J.* **90**, 4538-4545.

Milchev, A. and K. Binder, 1996, Dynamics of polymer chains confined in slit-like pores, *J. Phys. (Paris)* **6**, 21-31.

Nykypanchuk, D., H. H. Strey and D. A. Hoagland, 2002, Brownian motion of DNA confined within a two dimensional array, *Science* **297**, 987-990.

Nykypanchuk, D., H. H. Strey and D. A. Hoagland, 2005, Single molecule visualizations of polymer partitioning within model pore geometries, *Macromolecules* **38**, 145-150.

Odijk, T., 1977, Polyelectrolyte near rod limit, *J. Polym. Sci. B-Polym. Phys.* **15**, 477-483.

Odijk, T., 1983, On the statistics and dynamics of confined or entangled stiff polymers, *Macromolecules* **16**, 1340-1344.

Odijk, T., 2006, DNA confined in nanochannels: Hairpin tightening by entropic depletion, *J. Chem. Phys.* **125**, 204904.

Odijk, T. and A. C. Houwaart, 1978, Theory of excluded-volume effect of a polyelectrolyte in a 1-1 electrolyte solution, *J. Polym. Sci. B-Polym. Phys.* **16**, 627-639.

Olson, D. J., J. M. Johnson, P. D. Patel, E. S. G. Shaqfeh, S. G. Boxer and G. G. Fuller, 2001, Electrophoresis of DNA adsorbed to a cationic supported bilayer, *Langmuir* **17**, 7396-7401.

Perkins, T. T., S. R. Quake, D. E. Smith and S. Chu, 1994, Relaxation of a single DNA molecule observed by optical microscopy, *Science* **264**, 822-826.

Perkins, T. T., D. E. Smith, R. G. Larson and S. Chu, 1995, Stretching of a single tethered polymer in a uniform-flow, *Science* **268**, 83-87.

Randall, G. C., 2006, Single molecule analysis of DNA electrophoresis in microdevices, Ph.D. thesis.

Randall, G. C. and P. S. Doyle, 2004, Electrophoretic collision of a DNA molecule with an insulating post, *Phys. Rev. Lett.* **93**, 058104.

Randall, G. C. and P. S. Doyle, 2005a, DNA deformation in electric fields: DNA driven past a cylindrical obstruction, *Macromolecules* **38**, 2410-2418.

Randall, G. C. and P. S. Doyle, 2005b, Permeation-driven flow in poly(dimethylsiloxane) microfluidic devices, *Proc. Natl. Acad. Sci. USA* **102**, 10813-10818.

Randall, G. C. and P. S. Doyle, 2006, Collision of a DNA polymer with a small obstacle, *Macromolecules* **39**, 7734-7745.

Randall, G. C., K. M. Schultz and P. S. Doyle, 2006, Methods to electrophoretically stretch DNA: microcontractions, gels, and hybrid gel-microcontraction devices, *Lab Chip* **6**, 516-525.

Reisner, W., J. P. Beech, N. B. Larsen, H. Flyvbjerg, A. Kristensen and J. O. Tegenfeldt, 2007, Nanoconfinementenhanced conformational response of single DNA molecules to changes in ionic environment, *Phys. Rev. Lett.* **99**, 058302.

Reisner, W., K. J. Morton, R. Riehn, Y. M. Wang, Z. N. Yu, M. Rosen, J. C. Sturm, S. Y. Chou, E. Frey and R. H. Austin, 2005, Statics and dynamics of single DNA molecules confined in nanochannels, *Phys. Rev. Lett.* **94**, 196101.

Riehn, R., M. C. Lu, Y. M. Wang, S. F. Lim, E. C. Cox and R. H. Austin, 2005, Restriction mapping in nanofluidic devices, *Proc. Natl. Acad. Sci. USA* **102**, 10012-10016.

Rivetti, C., M. Guthold and C. Bustamante, 1996, Scanning force microscopy of DNA deposited onto mica: equilibration versus kinetic trapping studied by statistical polymer chain analysis, *J. Mol. Biol.* **264**, 919-932.

Rubinstein, M. and R. H. Colby, 2003, Polymer physics, Oxford University Press, Oxford ; New York.

Rybenkov, V. V., N. R. Cozzarelli and A. V. Vologodskii, 1993, Probability of DNA knotting and the effective diameter of the DNA double helix, *Proc. Natl. Acad. Sci. USA* **90**, 5307-5311.

Sakaue, T. and E. Raphael, 2006, Polymer chains in confined spaces and flow-injection problems: Some remarks, *Macromolecules* **39**, 2621-2628.

Salieb-Beugelaar, G. B., J. Teapal, J. Van Nieuwkasteele, D. Wijnperle, J. O. Tegenfeldt, F. Lisdat, A. van den Berg and J. C. T. Eijkel, 2008, Field-dependent DNA mobility in 20 nm high nanoslits, *Nano Lett.* **8**, 1785-1790.

Savin, T. and P. S. Doyle, 2005, Static and dynamic errors in particle tracking microrheology, *Biophys. J.* **88**, 623-638.

Shaqfeh, E. S. G., 2005, The dynamics of single-molecule DNA in flow, *J. Non-Newtonian Fluid Mech.* **130**, 1-28.

Shaw, S. Y. and J. C. Wang, 1993, Knotting of a DNA chain during ring-closure, *Science* **260**, 533-536.

Skolnick, J. and M. Fixman, 1977, Electrostatic persistence length of a wormlike polyelectrolyte, *Macromolecules* **10**, 944-948.

Stein, D., F. H. J. van der Heyden, W. J. A. Koopmans and C. Dekker, 2006, Pressure-driven transport of confined DNA polymers in fluidic channels, *Proc. Natl. Acad. Sci. USA* **103**, 15853-15858.

Stigter, D., 1977, Interactions of highly charged colloidal cylinders with applications to double-stranded DNA, *Biopolymers* **16**, 1435-1448.

Tang, J. and P. S. Doyle, 2007, Electrophoretic stretching of DNA molecules using microscale t junctions, *App. Phys. Lett.* **90**, 224103.

Teclemariam, N. P., V. A. Beck, E. S. G. Shaqfeh and S. J. Muller, 2007, Dynamics of DNA polymers in post arrays: Comparison of single molecule experiments and simulations, *Macromolecules* **40**, 3848-3859.

Tegenfeldt, J. O., C. Prinz, H. Cao, S. Chou, W. W. Reisner, R. Riehn, Y. M. Wang, E. C. Cox, J. C. Sturm, P. Silberzan and R. H. Austin, 2004a, The dynamics of genomic-length DNA molecules in 100-nm channels, *Proc. Natl. Acad. Sci. USA* **101**, 10979-10983.

Tegenfeldt, J. O., C. Prinz, H. Cao, R. L. Huang, R. H. Austin, S. Y. Chou, E. C. Cox and J. C. Sturm, 2004b, Micro- and nanofluidics for DNA analysis, *Analytical and Bioanalytical Chemistry* **378**, 1678-1692.

Teraoka, I., 1996, Polymer solutions in confining geometries, *Prog. Polym. Sci.* **21**, 89-149.

Turner, S. W. P., M. Cabodi and H. G. Craighead, 2002, Confinement-induced entropic recoil of single DNA molecules in a nanofluidic structure, *Phys. Rev. Lett.* **88**, 128103.

Ubbink, J. and T. Odijk, 1999, Electrostatic-undulatory theory of plectonemically superooiled DNA, *Biophys. J.* **76**, 2502-2519.

Usta, O. B., A. J. C. Ladd and J. E. Butler, 2005, Lattice-boltzmann simulations of the dynamics of polymer solutions in periodic and confined geometries, *J. Chem. Phys.* **122**, 094902.

Volkmuth, W. D. and R. H. Austin, 1992, DNA electrophoresis in microlithographic arrays, *Nature* **358**, 600-602.

Volkmuth, W. D., T. Duke, M. C. Wu, R. H. Austin and A. Szabo, 1994, DNA electrodiffusion in a 2d array of posts, *Phys. Rev. Lett.* **72**, 2117-2120.

Vologodskii, A. and N. Cozzarelli, 1995, Modeling of long-range electrostatic interactions in DNA, *Biopolymers* **35**, 289-296.

Wall, F. T., W. A. Seitz, J. C. Chin and P. G. de Gennes, 1978, Statistics of self-avoiding walks confined to strips and capillaries, *Proc. Natl. Acad. Sci. USA* **75**, 2069-2070.

Wang, Y. M., J. O. Tegenfeldt, W. Reisner, R. Riehn, X. J. Guan, L. Guo, I. Golding, E. C. Cox, J. Sturm and R. H. Austin, 2005, Single-molecule studies of repressor-DNA interactions show long-range interactions, *Proc. Natl. Acad. Sci. USA* **102**, 9796-9801.

Yamakawa, H., 1967, Modern Theory of Polymer Solutions, Harper and Row, New York.

Yang, Y. Z., T. W. Burkhardt and G. Gompper, 2007, Free energy and extension of a semiflexible polymer in cylindrical confining geometries, *Phys. Rev. E* **76**, 011804.

Zhang, C., F. Zhang, J. A. van Kan and J. R. C. van der Maarel, 2008, Effects of electrostatic screening on the conformation of single dna molecules confined in a nanochannel, *Journal of Chemical Physics* **128**, 225109.